Effects of doping on the magnetic anisotropy energy in $SmCo_{5-x}Fe_x$ and $YCo_{5-x}Fe_x$

P. Larson, I. I. Mazin, and D. A. Papaconstantopoulos
Center for Computational Materials Science, Naval Research Laboratory, 4555 Overlook Avenue SW, Washington, DC 20375-5320, USA

(Received 23 May 2003; revised manuscript received 18 November 2003; published 5 April 2004)

$SmCo_5$ is a technologically important material, having one of the largest magnetic anisotropy energies (MAE) of any hard magnet system. Common dopants include Fe and Cu, which produce grain boundaries that align individual grains, but also unintentionally dope the material within the grains. We have studied the magnetic properties of $SmCo_{5-x}Fe_x$ and $YCo_{5-x}Fe_x$ using density-functional theory calculations where the Sm $4f$ bands are treated within the LDA+U formalism (LDA—local-density approximation). Both supercell and virtual-crystal approximation calculations were performed for a series of Fe dopings. A strongly nonmonotonic behavior was found in the MAE for both series of compounds. The MAE of $SmCo_{5-x}Fe_x$ with $\sim 3-4$ % doping and of $YCo_{5-x}Fe_x$ with $\sim 6-7$ % doping increase by about 1 meV/f.u. before falling rapidly with larger Fe dopings. In both these cases, the results can be related to the position of the Fermi level with respect to the Co $3d$ minority peak in the density of states.

DOI: 10.1103/PhysRevB.69.134408 PACS number(s): 75.30.Gw, 75.20.Hr, 71.20.−b, 61.72.Ww

The magnetic properties of the permanent magnet intermetallic compounds $RECo_5$ (RE = rare earth) (specifically YCo_5 and $SmCo_5$) remain of high interest both experimentally[1,2] and theoretically.[3–12] The interest in these materials is fueled by their large magnetic anisotropy energy (MAE), which is defined as the difference between the ground-state energies due to rotation of the magnetic field (magnetization direction). While the main source of the large MAE in $SmCo_5$ and other Sm-Co magnets is the large magnetic single-site anisotropy of the Sm $4f$ shell,[9,12–15] the effects of the Co $3d$ states are an integral feature of this large anisotropy.

Sm-Co materials are important for hard magnet applications, thanks to their large coercivities, which depend on both the microscopic characteristics, such as the MAE or saturation magnetization, and on the microstructure of the actual material.[16] A common way to improve the microstructural properties is doping with 5–20 % Cu or Fe. Such doping leads to the formation of different phases at the grain boundaries, better alignment of the individual grains, and enhanced coercivity and remanence.[17] However, these dopants also diffuse in the bulk of the individual grains and affect the magnetic moments and MAE. In this paper we will study such effects on $SmCo_5$ doped with Fe using first-principles density-functional calculations. (Cu is nonmagnetic and will reduce the magnetic properties, so it will not be studied.)

The MAE of $SmCo_5$ comes from two main sources, the anisotropy of the localized Sm $4f$ shell[11,12] and a smaller contribution from the anisotropy of the itinerant Co $3d$ electrons.[11] The former contribution to the MAE arises from the interplay of the spin-orbit interaction within the Sm $4f$ shell with the crystal field on the Sm site. It is conceivable that adding Fe could change the crystal field, although the fact that Fe and Co are close neighbors makes this unlikely. To understand the effect of Fe doping on the MAE, it is instructive to compare $SmCo_{5-x}Fe_x$ with $YCo_{5-x}Fe_x$ which has no f electrons but does have a very similar structure of the Co $3d$ electrons. Indeed, one can show that the density of states (DOS) near the Fermi level is quite similar in both compounds, and that the relatively high MAE of the Co $3d$ electrons is related to a particular peak in the DOS at the Fermi level present in both compounds.[12] As discussed below, the effect of the Fe doping on the MAE is qualitatively the same in $SmCo_{5-x}Fe_x$ and $YCo_{5-x}Fe_x$ and is directly related to the Fermi-level shift due to the hole doping associated with Fe impurities.

We have performed a series of density-functional theory (DFT) calculations to study the MAE of the $SmCo_{5-x}Fe_x$ and $YCo_{5-x}Fe_x$ systems. $SmCo_{5-x}Fe_x$ and $YCo_{5-x}Fe_x$ are stable under normal preparation conditions only for $x \lesssim 1-1.5$.[18] However, all range of Fe replacements, up to 100%, can be studied within our calculations. A measurement of the MAE in $YCo_{5-x}Fe_x$ found an increase of $\gtrsim 0.5$ meV/f.u. around $x \lesssim 10\%$, although only four data points were examined.[19,20] We find that the MAE increases sharply by ~ 1 meV/f.u. in $YCo_{5-x}Fe_x$ with $x \sim 6-7$ % and for $SmCo_{5-x}Fe_x$ with $x \sim 3-4$ %. Since this is seen in both Y and Sm compounds, this initial increase cannot be due to the Sm $4f$-shell interacting with the changed crystalline environment, but is due to the MAE coming from the Co sublattice and changes in the position of the Fermi level. The MAE decreases rapidly with larger Fe concentrations. However, the dependence of the MAE on Fe concentration for the two systems are not simply related by a constant shift, indicating the increasingly important effect of Fe doping on the Sm-site crystal field. In this paper we present a systematic analysis of the effects of Fe doping on the MAE of these compounds using DFT calculations, as described below.

In our electronic structure calculations we have used the self-consistent, full-potential, relativistic, linearized augmented plane-wave (FLAPW) method.[21] The generalized gradient approximation of Perdew, Burke, and Ernzerhof[22] was used for the correlation and exchange potentials. Calculations were performed using the WIEN2K package.[23] A well converged basis consisting of ≈ 3000 LAPW basis functions was used with the Y and Sm sphere radii set to 2.115 a.u. and the Co sphere radii set to 2.015 a.u.. The results varied only

within a few percent for reasonable choices of atomic radii (2.0–3.0 a.u.). Local-orbital extensions[24] were included in order to accurately treat the upper core states and to relax any residual linearization errors. The plane-wave cutoff parameters RK_{max} and G_{max} were chosen as 9 and 14, respectively. Further increase of the cutoff parameters in YCo_5 (Ref. 11) did not to change the results in an appreciable way. Spin-orbit (SO) interaction was incorporated using a second-variational procedure,[25] where all states below the cutoff energy 1.5 Ry were included. This code includes the so-called $p_{1/2}$ extension,[21,26] which accounts for the finite character of the wave function at the nucleus for the $p_{1/2}$ state that cannot be adequately represented as a linear combination of a finite number of solutions of the radial Schrödinger equation with $l=1$.

Some previous calculations for the MAE of transition metals used the orbital polarization corrections (OPC) to improve agreement with experiment.[27] However, it is unclear how, if it is even possible, to include OPC together with LDA+U (LDA—local-density approximation). We chose to use LDA+U corrections instead for the following reasons. First, we believe that the physical justification for the LDA+U method is much stronger than for the OPC. Second, and more important, LDA+U corrects the positions of the f bands, while the OPC does not. LDA+U corrections were included for the Sm $4f$ shell using the fully localized prescription for the double-counting subtraction.[28] The earlier version of LDA+U included in the WIEN2K package[23] added the Hubbard correction *before* solving the second-variational spin-orbit equations, while the most recent version adds these terms *simultaneously*. The earlier prescription gave results dependent on such internal parameters as the size of the muffin-tin spheres and cutoff energies, but the latter prescription showed no dependence of these parameters within a reasonable range of values. The values of U and J used were 5 eV and 0.8 eV, respectively. The spin moment for Sm is $4.70\mu_B$ and per Co is $1.58\mu_B$. The orbital moment of Sm, $-2.8\mu_B$, is antiparallel to its spin moment, while the orbital moment of Co, $\sim 0.1\mu_B$/atom, is parallel to the Co spin moment. As will be shown later, the Sm $4f$ orbitals lie far from the Fermi level, and the value of the Sm spin and orbital moments remain unchanged with Fe doping. Therefore, the Sm $4f$ orbitals do not play a role in the *change* of the MAE with Fe doping on the Co sites, so remaining details of the LDA+U effects on Sm can be found in our previous paper.[12] Interestingly, including both spin-orbit and LDA+U corrections appear essential not only for the orbital magnetization but also for the spin magnetization. While nonrelativistic LDA+U calculations or relativistic open-core calculations converge to a ferrimagnetic arrangement of spin moments (the mechanism of this phenomenon was described, for instance, by Brooks *et al.*[29]), simultaneous inclusion of both effects renders this solution unstable, and the ground state is characterized by parallel alignment of the Co and Sm spin moments, improving the agreement with experiment (total magnetization of $9.9\mu_B$ compared to the experimental value of $8.9\mu_B$).[30,31]

This ferromagnetic configuration of the Sm and Co spins differs from the ferrimagnetic configuration seen in related

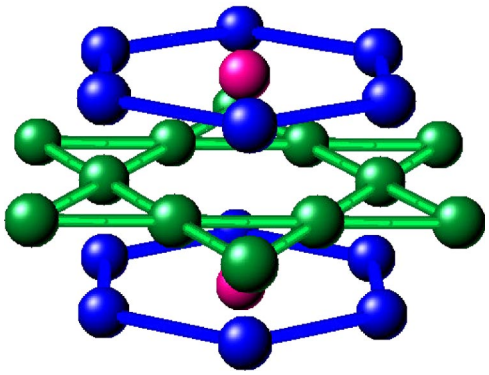

FIG. 1. Crystal structure of $SmCo_5$. Sm (or Y) lies in the middle of the hexagonal Co(2c) layers, while the Co($3g$) lattice forms a Kagome lattice in the XY plane.

rare-earth compounds (but not directly measured in $SmCo_5$) (Ref. 32) as well as from calculations of YCo_5 (Refs. 11 and 12) where the Y and Co moments are antiparallel. This may indicate a problem in the LDA+U formalism itself, or it may be that the moments in $SmCo_5$ are indeed parallel, differing from the generally accepted view for similar compounds.[32] We find good agreement with the MAE and total moment in $SmCo_5$, which provides indirect evidence for the latter choice. This is particularly true of the total moment, since the MAE is mainly determined by the filling of the Co $3d$ band and the crystal field at the Sm site, neither of which is much affected by the direction of the magnetization on Sm. Note that mutual orientation of Sm and Co moments depends on the energy balance of several factors, such as Sm $4d$–Co $3d$ hybridization, filling of the Co bands, and direct Sm $4f$–Co $3d$ hybridization.[33] In any event, this suggests the need for further experimental and theoretical studies of this material.

The crystal structure of $SmCo_5$ and YCo_5 is that of $CaCu_5$, $P6/mmm$. The experimental values of a and c/a used in the calculation are 9.452 a.u. and 0.792 a.u. for $SmCo_5$ and 9.313 a.u. and 0.806 for YCo_5.[34] The Co sites are separated into two sets of inequivalent atoms, Co(2c) having twofold multiplicity and Co($3g$) having threefold multiplicity (Fig. 1). Including spin-orbit coupling into the calculation lowers the symmetry, when the field lies along the plane, to $Pmmm$, separating the three atoms corresponding to Co($3g$) into two inequivalent sites that have multiplicities of 2 and 1, respectively (without changing the unit-cell volume). In the following we will refer to these sites as $Co_2(3g)$ and $Co_1(3g)$ (Fig. 1). To eliminate any systematic errors[11] we performed the calculation for both magnetization directions using the same, highest *common* symmetry group, $Pmmm$.[34]

An important consideration is the number of **k** points necessary to properly converge the MAE. Some calculations of YCo_5[4] could not find convergence even with several thousand **k** points in the irreducible Brillouin zone. Other calculations of the MAE in YCo_5[7,10] found that the MAE changed by only about 0.1 meV/f.u. when going from ~ 60 to $\sim 15\,000$ **k** points in the irreducible Brillouin zone. More variation was found when orbital polarization corrections

were included,[7,10] which has not been considered in this paper. We found earlier[11] that our values for MAE are reasonably converged with an $8\times8\times8$ mesh, corresponding to 600 **k** points in the full Brillouin zone. Stepping up to a $10\times10\times11$ mesh (1200 **k** points) changed the MAE by only ~0.1 meV/f.u. The following factors have possibly contributed to a rapid convergence, although we did not investigate the relative importance of these factors. First, using the Bloechl modified tetrahedron scheme had already been observed[7] to give a substantial improvement over the standard tetrahedron method.[4] Second, as we pointed out in our previous paper,[11] calculations of the MAE in the full-symmetry unit cell converges very slowly while convergence is much faster when the same low symmetry is used for both magnetization directions. Finally, it is possible that using full self-consistent calculations, as opposed to the force theorem, may provide a better convergence, although we have not tested this assumption.

Within the chosen symmetry, one can perform supercell calculations in Y(or Sm)$Co_{5-x}Fe_x$ for integer values of x. There are two possible configurations of Fe and Co atoms for $x=2$ and $x=3$ within this symmetry [with Co or Fe in either the Co(2c) or $Co_2(3g)$ site], both configurations giving similar, albeit not identical, results for the MAE and magnetic moments. For small dopings ($x<1$) one can use the virtual-crystal approximation, where a virtual atom with $\mathbf{Z}=27-x$ is placed at the $Co_1(3g)$ site. This is not only convenient computationally, but also is consistent with experimental evidence[31,35,36] that Fe impurities prefer the Co(3g) sites, which are slightly bigger (the atomic radius of Fe is larger than that of Co), and consistent with total-energy calculations within DFT.[10] We performed structural relaxation of the volumes and c/a ratios (the internal parameters are set by symmetry) for several different configurations of $YCo_{5-x}Fe_x$ and $SmCo_{5-x}Fe_x$. In pure YCo_5 and $SmCo_5$ the calculated volume and c/a ratio practically coincide with the experimental values listed above. For the Fe doped compounds, the calculated c/a ratio interestingly remains the same as in the pure compounds, within the accuracy of the calculations, while the volume increases very little, a maximum of up to 4% for large Fe concentrations. While we used the optimized crystal structure for calculating the MAE, the differences from the undoped structures are so insignificant that the calculation can be performed as well in the same structure for all compositions.

Our results for the total magnetic moment are shown in Fig. 2, together with the previous calculation.[10] We find, as expected, a monotonic increase of magnetization with Fe concentration up to $x=4$, but a small reduction for YFe_5 compared to $YCoFe_4$. Similar dependence is found in $SmCo_{5-x}Fe_x$. Interestingly, the previous attempt to investigate the effect of Fe on the magnetic moment in $YCo_{5-x}Fe_x$[10] found a local minimum at $x=3$. Steinbeck *et al.*[10] used a full-potential linear combination of atomic orbitals (LCAO) method, as opposed to the full-potential LAPW method that we have employed. The ways of treating the nonspherical corrections in these two methods are very different. We verified, however, that the difference is not due to the nonspherical part by performing a linearized muffin-tin orbital calculation within the atomic sphere approximation (LMTO-ASA) using the STUTTGART-4.7 package[37] (Fig. 2), which agrees very well with the LAPW results. The origin of the disagreement with the LCAO calculation,[10] therefore, remains unclear.

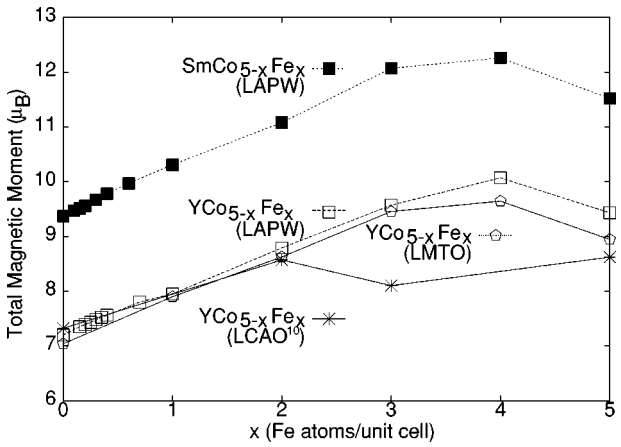

FIG. 2. Total magnetic moments per unit cell calculated for different Fe concentrations x in $SmCo_{5-x}Fe_x$ and $YCo_{5-x}Fe_x$ using LAPW. Our LMTO results and the previous LCAO result (Ref. 10) for $YCo_{5-x}Fe_x$ are also given.

The downturn in the moments seen in both $YCo_{5-x}Fe_x$ and $SmCo_{5-x}Fe_x$ between $x=4$ and $x=5$ seems strange, because Fe is, generally speaking, a more magnetic element than Co. This result is similar to that seen in Fe-Co alloys (the so-called Slater-Pauling curve[38]), which was explained by the variation of the density of states in the rigid-band model. However, the Slater-Pauling curve is not directly applicable to $YCo_{5-x}Fe_x$ and $SmCo_{5-x}Fe_x$. Indeed, the crystal structure of the Co sublattice in YCo_5 is very different from that of the elemental Co and Fe, and so is the density of states. However, the general idea that the downturn is not due to a change in the Stoner parameter, but rather to the structure of the DOS, does apply to our systems. To illustrate this quantitatively, we use the so-called extended Stoner model,[39] which can be viewed as a special case of Andersen's force theorem.[40] The latter states the total-energy difference resulting from a change in the external potential is given, to second order in the charge perturbation, by the difference in the sum of the one-electron energies as long as the energy density is *not* recalculated self-consistently.[40] If the external potential change is just an external magnetic field, this theorem calls for a rigid splitting of the spin-up the spin-down states. This results in a loss of the one-electron energy equal to

$$\frac{1}{2}\int_0^m \frac{m\,dm}{\tilde{N}(m)}, \tag{1}$$

where m is the induced magnetization and $\tilde{N}(m)$ is the appropriately averaged DOS.[39] This energy loss is offset by the magnetic (Hund's rule) energy, usually quantified as $-m^2I/4$, where I is the atomiclike Stoner parameter. The parameter I is an atomic characteristic, very weakly depen-

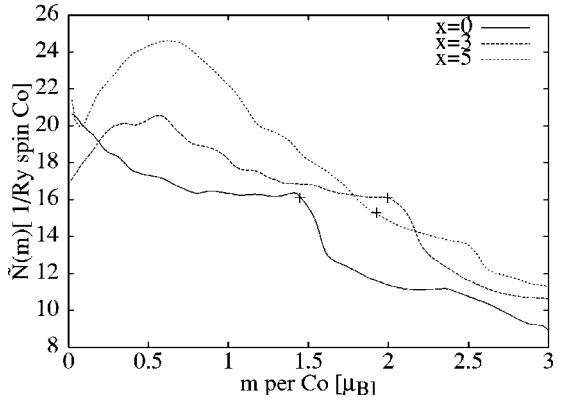

FIG. 3. Extended Stoner calculations (see text) for YCo_5, YCo_2Fe_3, and YFe_5. Effective DOS's were obtained from the LMTO-ASA calculations. Crosses show the equilibrium magnetizations obtained with the same setup. The corresponding values of the Stoner *I*, required to obtain the self-consistent magnetization values, are 0.85, 0.84, and 0.89 eV, respectively.

dent on the crystallographic environment. The total-energy difference between the magnetic and nonmagnetic state is, therefore, expressed as

$$\Delta E(m) = \frac{1}{2}\int_0^m \frac{m\,dm}{\tilde{N}(m)} - \frac{I\,m^2}{4}. \qquad (2)$$

Stable or metastable magnetic configurations are found when $I\tilde{N}(m)=1$ and $d\tilde{N}(m)/dm<0$. We show the dependence of $\tilde{N}(m)$ on m for three representative Fe concentrations in Fig. 3. For $YCo_{5-x}Fe_x$ the composite Stoner factor is defined as $I=(5-x)I_{Co}(N_{Co}/N)^2+xI_{Fe}(N_{Fe}/N)^2$, where N and $N_{Fe(Co)}$ denote the total and the partial densities of states at the Fermi level. The composition of the bands at the Fermi level may, in principle, change with the concentration and so may the composite Stoner factor. One can make a plausible assumption that the loss of the magnetization at high Fe concentrations is due to a decrease in the Stoner *I*. However, Fig. 3 shows that practically the same *I* is needed for all three concentrations to reproduce the self-consistent magnetizations within the extended Stoner theory. The nonmonotonic dependence of the equilibrium magnetization, therefore, is a result of the systematic change in the DOS upon Fe doping.

We shall now turn to the effect of doping on the MAE. Almost no experimental information exists on this important subject. Limited data exists for $YCo_{5-x}Fe_x$ with $x\approx 0$, 0.5, 0.8, and 1.4,[19] and none, to the best of our knowledge, for $SmCo_{5-x}Fe_x$. Similarly, first-principles calculations have been reported[10] for $YCo_{5-x}Fe_x$ with $x=0$, 2, 3, and 5, and none for $SmCo_{5-x}Fe_x$. Franse *et al.*[19] observed that the MAE increased from $x=0$ to $x\approx 0.5$ and then decreased for larger *x*. On the other hand, Steinbeck *et al.*[10] studied larger doping levels where their calculations found the MAE decreased to zero for YCo_3Fe_2, with a small increase upon adding another Fe, and an ultimate drop to a negative value in pure YFe_5. There is no way of comparing these calculations with experiment, because their first calculated point is already out of the range of experimental studies. However,

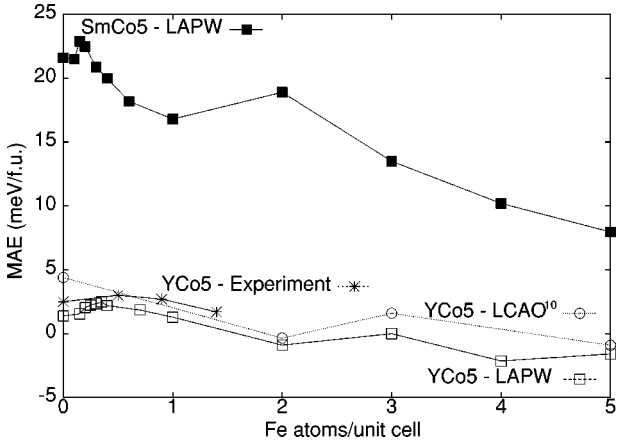

FIG. 4. Calculated MAE in $YCo_{5-x}Fe_x$ and $SmCo_{5-x}Fe_x$ as a function of *x* using LAPW. The maximum MAE is obtained for $x\sim 0.35$ for $YCo_{5-x}Fe_x$ and ~ 0.15 for $SmCo_{5-x}Fe_x$. The experimental values (Ref. 19) and previous LCAO results (with orbital polarization correction) (Ref. 10) for the MAE in $YCo_{5-x}Fe_x$ are also given.

our calculations, which cover both small dopings [using the virtual-crystal approximation (VCA)] and large dopings (using supercells), compare favorably both with the experiment[19] and with the points calculated by Steinbeck *et al.*[10] (Fig. 4). We find an initial increase of the MAE with a maximum at $x\approx 0.35$, consistent with the experiment,[19] and a substantial nonmonotonic drop of the MAE at $x>1$. While there is no easy way to gauge the reliability of the VCA for MAE calculations, our VCA curve connects continuously with the supercell curve (Fig. 4), suggesting that this approximation is not too bad here. We will show below that the MAE is strongly dependent on the position of the Fermi level, so that much of the physics involved can be understood within the rigid-band approximation which explains this unexpected success of the VCA. As mentioned earlier, the two calculated curves for $YCo_{5-x}Fe_x$ and $SmCo_{5-x}Fe_x$ are not related by a simple constant shift (Fig. 4), indicating that the Fe dopants somewhat affect the Sm crystal field.

Comparing our calculations for the MAE of $YCo_{5-x}Fe_x$ and $SmCo_{5-x}Fe_x$ (Fig. 4), we see that the behavior is qualitatively similar, especially at small dopings: an initial increase followed by a rapid, but nonmonotonic, decay. While $YCo_{5-x}Fe_x$ and $SmCo_{5-x}Fe_x$ can only be produced for $x\lesssim 1-1.5$,[18] the change of the easy axis in $YCo_{5-x}Fe_x$ from the *c* axis to the in-plane direction is consistent with what has been observed for $ThCo_5$ to $ThFe_5$.[19] However, in $SmCo_{5-x}Fe_x$ the large MAE associated with the Sm $4f$ electrons prevents the change of sign of the total MAE. We conclude that these qualitative features are likely to be associated with the Co $3d$ electrons.

To gain more insight in this, we turn again to the force theorem.[40] This theorem cannot be directly applied to $SmCo_{5-x}Fe_x$ since the spin-orbit interaction forces the Sm $4f$ shell to rotate with magnetic field, and the resulting change in (spin) density is not small. However, one can apply this theorem to $YCo_{5-x}Fe_x$ by comparing the total ener-

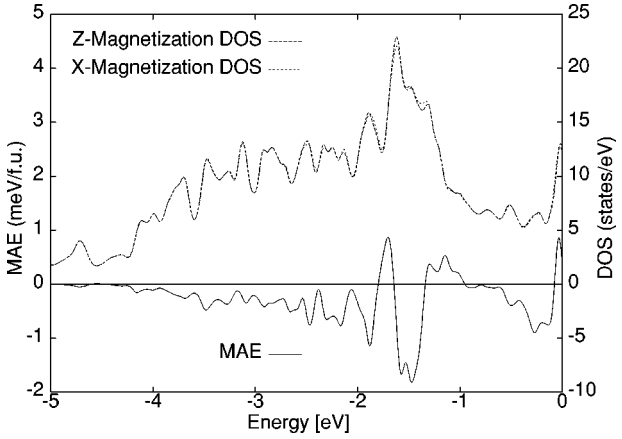

FIG. 5. The calculated DOS's of YCo_5 for the magnetic field along X and Z field directions are nearly indistinguishable on this scale, shown here along with the running value of the MAE calculated by the force theorem. Note the contribution coming from the peak close to the Fermi level.

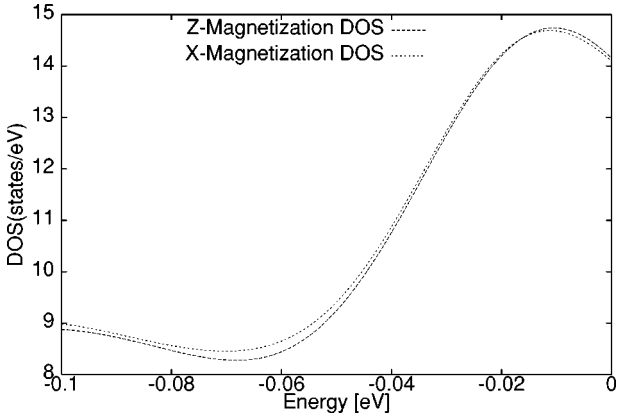

FIG. 7. Calculated total DOS of $SmCo_5$ for the two field directions. While the force theorem cannot be applied in this case, the peak lies closer to the Fermi level. The similarity to the DOS for YCo_5 (Fig. 6) suggests that the calculated increase in the MAE is also related to the peak below the Fermi level.

gies calculated for the same charge and spin-density distribution, but with different directions of the external field, i.e.,

$$E_{\mathrm{MAE}} \approx \Sigma_i^{occ} \epsilon_i^X - \Sigma_i^{occ} \epsilon_i^Z = \int_{E<E_F} [N^X(E) - N^Z(E)] E dE, \tag{3}$$

where the indices X and Z show the direction of the field. We checked that the difference between the Fermi energies in the two calculations is insignificant. In Fig. 5 we show the last integral as a function of the upper integration limit. Also note that the largest difference between $N^X(E)$ and $N^Z(E)$ appears around $E \approx -1.5$ eV, but this difference is integrated out and does not manifest itself in the MAE. The majority of the nonzero component of integral (3) is collected in the vicinity of the Fermi level, where small changes in the peak in the DOS [which has mostly Co(2c) $3d$ character] result in sizable changes in the MAE. [Polarized neutron studies have shown that the large anisotropy in $RECo_5$ compounds arises from the Co(2c) site,[41,42] which has been confirmed by point-charge calculations.[43])] This mechanism is most effective when the Fermi level is situated right at the top of the X-magnetization direction peak, so that $N^X(E) - N^Z(E)$ is positive below and negative above the Fermi level. In pure YCo_5 this maximum in the DOS is slightly below the Fermi level (Fig. 6). The main effect of a small Fe doping is shifting the Fermi level down. Indeed, we find the Fermi level crosses the maximum of the X-magnetization direction DOS at $x \sim 0.3-0.4$, and this is precisely where we find the maximum of MAE (Fig. 6). A similar plot for $SmCo_5$ (Fig. 7) shows the corresponding Co(2c) $3d$-derived peak lies even closer to the Fermi level. Again, doping with Fe shifts the Fermi level to the maximum of the X-magnetization direction DOS peak, but now it happens at smaller Fe concentrations, again in agreement with the direct calculations of MAE.

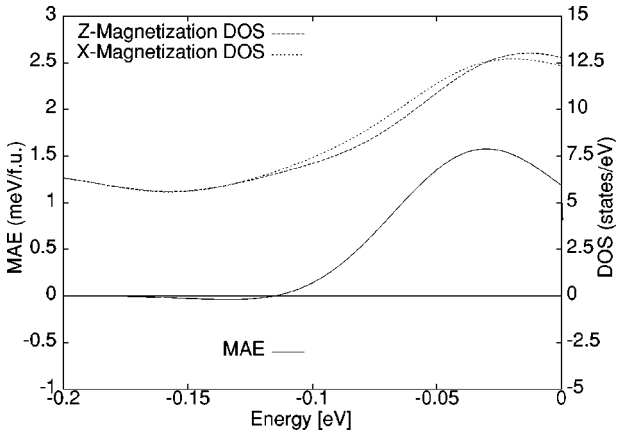

FIG. 6. Calculated DOS of YCo_5 for the Z and X field directions along with the running value of the MAE calculated by the force theorem, blown up to emphasize the region near the Fermi level.

To conclude, we have performed first-principles calculations of the magnetic properties of $YCo_{5-x}Fe_x$ and $SmCo_{5-x}Fe_x$ using a highly accurate LAPW code including the LDA+U corrections. The MAE shows a strongly nonmonotonic behavior for small values of doping with a sharp peak followed by a rapid decrease. The calculated MAE increased from 1.4 meV/f.u. in YCo_5 to 2.5 meV/f.u. for $YCo_{4.65}Fe_{0.35}$ and from 21.6 meV/f.u. for $SmCo_5$ to 22.5 meV/f.u. for $SmCo_{4.85}Fe_{0.15}$. In both of these cases, the maximum value in the MAE corresponds to concentrations where the Fermi level moves to the top of the Co(2c) $3d$ X-magnetization direction peak in the DOS. The change in the MAE agrees well with the limited experimental evidence,[19] though more detailed experiments are needed. Our calculations suggest that such a behavior of MAE is generic for all $RECo_{5-x}Fe_x$ compounds, and not just for $YCo_{5-x}Fe_x$ and $SmCo_{5-x}Fe_x$.

This work was supported by the Office of Naval Research and DARPA Grant No. 63-8250-02. We are grateful to A. Gabay and G. Hadjipanais for useful discussions.

[1] H.R. Kirchmayr and C.A. Poldy, J. Magn. Magn. Mater. **8**, 1 (1978).
[2] R.J. Radwanski and J.J.M. Franse, Int. J. Mod. Phys. **7**, 782 (1993).
[3] S.K. Malik, F.J. Arlinghaus, and W.E. Wallace, Phys. Rev. B **16**, 1242 (1977).
[4] L. Nordstrom, M.S.S. Brooks, and B. Johansson, J. Phys.: Condens. Matter **4**, 3261 (1992).
[5] J. Trygg, L. Nordstrom, and B. Johansson, *Physics of Transition Metals*, edited by P.M. Oppeneer and J. Kubler (World Scientific, Singapore, 1993), p. 745.
[6] M. Yamaguchi and S. Asano, J. Appl. Phys. **79**, 5952 (1996).
[7] G.H.O. Daalderop, P.J. Kelly, and M.F.H. Schuurmans, Phys. Rev. B **53**, 14 415 (1996).
[8] M. Yamaguchi and S. Asano, J. Magn. Magn. Mater. **168**, 161 (1997).
[9] L. Steinbeck, M. Richter, and H. Eschrig, J. Magn. Magn. Mater. **226-230**, 1011 (2001).
[10] L. Steinbeck, M. Richter, and H. Eschrig, Phys. Rev. B **63**, 184431 (2001).
[11] P. Larson and I.I. Mazin, J. Appl. Phys. **93**, 6888 (2003).
[12] P. Larson, I.I. Mazin, and D.A. Papaconstantopoulos, Phys. Rev. B **67**, 214405 (2003).
[13] M. Richter, P.M. Oppeneer, H. Eschrig, and B. Johansson, Phys. Rev. B **46**, 13 919 (1992).
[14] P. Novak and J. Kuriplach, IEEE Trans. Magn. **MAG-30**, 1036 (1994).
[15] K. Hummler and M. Fähnle, Phys. Rev. B **53**, 3272 (1996).
[16] J. Sort, S. Suriñach, J.S. Muñoz, M.D. Baró, J. Nogués, G. Chouteau, V. Skumryev, and G.C. Hadjipanayis, Phys. Rev. B **65**, 174420 (2002); J. Ding, P.G. McCormick, and R. Street, J. Magn. Magn. Mater. **135**, 200 (1994).
[17] J.C. Téllez-Blanco, R. Grössinger, and R. Sato Turtelli, J. Alloys Compd. **281**, 1 (1998).
[18] Z.D. Zhang, W. Liu, J.P. Liu, and D.J. Sellmyer, J. Phys. D **33**, R217 (2000).
[19] J.J.M. Franse, N.P. Thuy, and N.M. Hong, J. Magn. Magn. Mater. **72**, 361 (1988).
[20] F. Rothwarf, H.A. Leupold, J. Greedan, W.E. Wallace, and Dilip K. Das, Int. J. Magn. **4**, 267 (1973).
[21] D.J. Singh, *Planewaves, Pseudopotentials, and the LAPW Method* (Kluwer Academic, Boston, 1994).
[22] J.P. Perdew, K. Burke, and M. Ernzerhof, Phys. Rev. Lett. **77**, 3865 (1996).
[23] P. Blaha, K. Schwarz, G. K. H. Madsen, K. Kvasnicka, and J. Luitz, Computer code WIEN2K (Karlheinz Schwarz, Techn. Universitat Wien, Austria, 2001).
[24] D. Singh, Phys. Rev. B **43**, 6388 (1991).
[25] D.D. Koelling and B. Harmon, J. Phys. C **10**, 3107 (1977); P. Novak (unpublished).
[26] J. Kunes, P. Novak, R. Schmid, P. Blaha, and K. Schwarz, Phys. Rev. B **64**, 153102 (2001).
[27] P. Ravindran, A. Kjekshus, H. Fjellvag, P. James, L. Nordström, B. Johansson, and O. Eriksson, Phys. Rev. B **63**, 144409 (2001); P. Ravindran, A. Delin, P. James, B. Johansson, J.M. Wills, R. Ahuja, and O. Eriksson, *ibid.* **59**, 15 680 (1999).
[28] A.G. Petukhov, I.I. Mazin, L. Chioncel, and A.I. Lichtenstein, Phys. Rev. B **67**, 153106 (2003).
[29] M.S.S. Brooks, T. Gasche, S. Auluck, L. Nordström, L. Severin, J. Trygg, and B. Johansson, J. Appl. Phys. **70**, 5972 (1991).
[30] T.-S. Zhao, H.-M. Jin, G.-H. Gua, X.-F. Han, and H. Chen, Phys. Rev. B **43**, 8593 (1991).
[31] J. Déportes, D. Givord, J. Schweizer, and F. Tasset, IEEE Trans. Magn. **MAG-12**, 1000 (1976).
[32] K.H.J. Buschow, Rep. Prog. Phys. **40**, 1179 (1977).
[33] The standard explanation of the antiparallel alignment of the transition-metal (TM) and rare-earth (RE) magnetic moments is based on the following consideration. First, hybridization between the RE *f* states and TM *d* states is neglected. Second, hybridization of the high-lying, empty RE *d* bands and the partially occupied TM *d* bands is taken into account as a perturbation, which admixes RE *d* states into the TM *d* bands. Since the spin-majority TM *d* states are lower in energy than the spin-minority states, the energy distance between the unperturbed RE and TM *d* bands is larger in the majority channel and therefore the mixing is weaker. The amount of RE *d* states admixed in the TM *d* bands is of the order of $t^2/(E_{RE\text{-}d}-E_{\uparrow(\downarrow)})^2$, where *t* characterizes the hopping amplitude between the RE and TM *d* orbitals, $E_{RE\text{-}d}$ is the energy of the RE *d* states, and $E_{\uparrow(\downarrow)}$ is the center of gravity of the majority (minority) TM *d* band. Obviously, there will be more spin-minority RE *d* states mixed into TM *d* bands than spin-majority states, which means that the induced polarization in the RE *d* states is antiparallel to that of the TM *d* states. The RE *f* orbitals then align parallel to the RE *d* orbitals by Hund's first rule. This argument, however, leaves out two important issues. First, the spin-minority TM *d* band is only partially occupied, while the spin-majority band is fully occupied. The difference of the occupancies, $M=N_{\uparrow}-N_{\downarrow}$, is the TM *d* band contribution to the magnetization, which is about $1.5\mu_B$ in $SmCo_5$. Thus, even though each state in the spin-minority TM *d* band has more RE *d* character than the corresponding state in the spin-minority band, the total amount of the RE *d* admixture is defined by $N_{\uparrow(\downarrow)}t^2/(E_{RE\text{-}d}-E_{\uparrow(\downarrow)})^2$, and is not necessarily larger in the spin-minority channel. It is easy to estimate that the antiparallel alignment takes place only when $(E_{\downarrow}-E_{\uparrow})/(E_{RE\text{-}d}-E_{TM\text{-}d})>M/2N_{\uparrow}\approx M/10$. Since the exchange splitting $(E_{\downarrow}-E_{\uparrow})\approx IM$, where *I* is the Stoner factor of the order of 1 eV, we roughly estimate that $E_{RE\text{-}d}-E_{TM\text{-}d}$ should be less than 10 eV to assure the antiparallel alignment. This is indeed the case in YCo_5 and $SmCo_5$, and we did find the antiparallel alignment in YCo_5 (Ref. 11). However, this mechanism substantially reduces the tendency to antiparallel alignment and makes room for the possibility that the hybridization between the RE *f* and TM *d* states in $SmCo_5$, which favors parallel alignment of the RE and TM moments, actually reverses the trend, as in our calculation for $SmCo_5$. Note that, contrary to a popular misconception, this hybridization is not negligibly small. One can show (Ref. 44) that up to 80% of the crystal-field splitting of the *f* states comes from hybridization.
[34] R.W.G. Wyckoff, *Crystal Structures* (Krieger, Melbourne, FL, 1986), Vol. 2.
[35] J. Laforest and J.S. Shah, IEEE Trans. Magn. **MAG-9**, 217 (1973).
[36] R.L. Streever, Phys. Rev. B **19**, 2704 (1979).
[37] O.K. Andersen, Tight-Binding LMTO, Ver. 4.7 (Max-Planck-

Institut für Festkörperforschung, Stuttgart, 1994).
[38] J. Kuebler, *Theory of Itinerant Electron Magnetism* (Clarendon Press, Oxford, 2000).
[39] G.L. Krasko, Phys. Rev. B **36**, 8565 (1987).
[40] O.K. Andersen, J. Madsen, U.K. Poulsen, O. Jepsen, and J. Kollar, Physica B & C **86**, 249 (1977).
[41] R.L. Streever, Phys. Rev. B **19**, 2704 (1979).
[42] J.M. Alameda, D. Givord, R. Lemaire, and Q. Lu, J. Appl. Phys. **52**, 2079 (1981).
[43] K. Inomata, Phys. Rev. B **23**, 2076 (1981).
[44] P. Larson, I.I. Mazin, and D.A. Papaconstantopoulos, Phys. Rev. B **69**, 012404 (2004).